PHYSICAL REVIEW A **75**, 030902(R) (2007)

Atom trap with surface plasmon and evanescent field

C. García-Segundo,[1,2] H. Yan,[1,2,3] and M. S. Zhan[1,2]
[1]*State Key Laboratory of Magnetic Resonance and Atomic and Molecular Physics, Wuhan Institute of Physics and Mathematics, Chinese Academy of Sciences, Wuhan 430071, People's Republic of China*
[2]*Center for Cold Atom Physics, Chinese Academy of Sciences, Wuhan 430071, People's Republic of China*
[3]*Graduate School, Chinese Academy of Sciences, Beijing 100080, People's Republic of China*
(Received 8 November 2006; published 26 March 2007)

We propose the use of a structured planar mirror as the way to obtain the physical conditions for which the combination of an evanescent field and a surface plasmon potential would result in an atom-trap well located at ~0.6 μm above the mirror's surface. We present calculations from which we obtain a well depth slightly bigger than 7 μK. The configuration and calculations we present are for a single trap, however, there would appear to be no restrictions to extend this idea to a two-dimensional matrixlike array of traps, hinting on the possibility for tailored design of latticelike trap structures.

DOI: 10.1103/PhysRevA.75.030902 PACS number(s): 34.50.Dy, 73.20.Mf, 39.25.+k, 81.16.Ta

Since the pioneering work on simultaneously cooling and trapping atoms with lasers many other types of trap wells have been developed [1–4]. There is an increasing interest in trapping atoms near a surface [5], especially with the general aim of constructing three-dimensional (3D)-lattice-trap structures [6], with conditions to confine atoms at the required density and thus to realize an effective atom chip [7,8]. One of the main problems is to overcome the decoherence that the atoms would exhibit when these are set up on the atom lattice trap [9,10]. Already established atom-trap methods use electric currents and/or magnetic fields to confine atoms in two-dimensions and then manipulate the atoms along the third spatial dimension; however, the stability of the applied fields is limited by fluctuations, mainly of thermal origin, which ultimately result in decoherence [11]. The method known as the double-evanescent-wave (DEW) trap well, first put forward by Cook and Hill [12–15], suggested the use of evanescent fields (EFs) to produce atomic mirrors and manipulate neutral or degenerated atoms to be trapped near a surface of reference. Since the EF is a direct consequence of the coherence properties of an external field, it may be expected that with this method we can reach physical conditions to achieve the stable coherence required for the atom chip. In spite of the many efforts, however, the decoherence problems still remain; highlighting the difficulty of forming efficient lattice-well traps.

In this paper, we suggest the use of a structured atom mirror surface, and with it describe a method to achieve a stable well trap. We begin with the well-understood process of generating an enhanced evanescent field via total internal reflection (TIR). This occurs when light of appropriate frequency (ω) is incident from within an optically transparent dielectric prism at an angle θ slightly above the TIR critical angle θ_c, at the interface with the vacuum. For our purpose we require the frequency to be blue-detuned away from a suitable atomic resonance. The enhancement in the EF is obtained by adding to the surface of the prism a thin film of a highly conductive, nonmagnetic metal of a few tens of nanometers thickness, with resonant plasmon modes far away from the illumination frequency. The demonstration of the principle and its general description already exist in the literature [14–17]. We propose to include microsize spots of a second highly conductive and nonmagnetic metal of the same thickness. This time presenting the evanescent field together with active plasmon modes near the illumination frequency, so as to promote "soft" coupling with the EF (see Fig. 1). Consequently the atomic mirror potential shall be modified. When an atom in its ground state interacts with surface plasmon modes, the resulting effective potential has the steady attractive interaction found by Casimir and Polder. Instead, if the atom is in an excited state, the resulting interaction potential is quasioscillatory as a result of the retarded self-interaction of the atom's quantum charge fluctuations in the presence of the mirror. The strength of the resulting force will depend on the coherence conditions between the oscillation mode (plasmon) and the atom's excitation state; e.g., when these are mutually coherent, it will be of the same order of magnitude as the vacuum contribution, and under partial coherence it will be smaller [18]. Thus we look for coherence conditions such that the EF and the plasmon are balanced, without mutually canceling each other. This results in a potential well with stable equilibrium, above the active

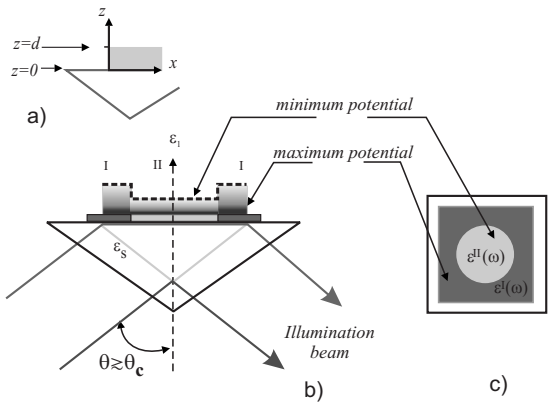

FIG. 1. Schematic representation of (a) the coordinates system. (b) The potential resulting from the enhanced evanescent field on the region I; and the potential resulting from the PF plus the EF on the region II. (c) Area of distribution of the metallic layers; the dielectric function, as indicated, establishes the correspondent potential. The scales are exaggerated for explanatory purposes only.

plasmon modes area [19] (region II in Fig. 1).

These EF and plasmon fields are obtained by solving Maxwell's wave equation, with the respective continuity boundary conditions for the N-involved media of isotropic and homogenous dielectric function ϵ_N, with $N=(1)$ for vacuum, $N=(m)$ for the metal layer, and $N=(s)$ for the dielectric substrate. Taking the mirror surface parallel to the (x,y)-plane, the resulting EF would extend along the z-coordinate; i.e., normal to that surface. While the plasmon mode propagates along the x-coordinate with wave vector $k_\parallel$, which is reduced from $c^2k_\parallel^2=\omega^2\epsilon_s \sin^2\theta$. Along the y-direction the resulting field has no component. Finally, the field output is a p-polarized (TM) electromagnetic field vector,

$$\boldsymbol{E}(\boldsymbol{k},\boldsymbol{r};t)=\left(\frac{k_{zN}}{k_o\epsilon_N}E_{xN},0,-\frac{k_\parallel}{k_o\epsilon_N}E_{zN}\right)e^{-k_{zN}z_N}e^{i(k_\parallel x-\omega t)}; \quad (1)$$

while the s-field's component produces no output. Once the illumination frequency is set, $k_o=\omega/c$ keeps constant (as c is the speed of the light). This term will not be mentioned again, however, it is considered for computation purposes. The resulting wave vector is $\boldsymbol{k}=(k_\parallel,0,k_N)$. The amplitudes E_{jN}, $j=x,z$ together with the wave numbers and the EF's depth of penetration into the vacuum will define the distance above the reference surface for the installation of the potential. The first task now is to obtain these amplitudes. This is achieved by applying standard boundary conditions to the system:

$$\boldsymbol{E}(k_\parallel,z\geqslant d;t)=\left(\frac{k_{z1}}{\epsilon_1}E_{x1},0,-\frac{k_\parallel}{\epsilon_1}E_{z1}\right)e^{-k_{z1}z_1}e^{i(k_\parallel x-\omega t)}, \quad (2)$$

$$\boldsymbol{E}(k_\parallel,0\leqslant z\leqslant d;t)=\left(\frac{k_{zm}}{\epsilon_m}E_{xm},0,-\frac{k_\parallel}{\epsilon_m}E_{zm}\right)e^{-k_{zm}z_m}e^{i(k_\parallel x-\omega t)}, \quad (3)$$

$$\boldsymbol{E}(k_\parallel,z\leqslant 0;t)=\left(\frac{k_{zs}}{\epsilon_s}E_{xs},0,-\frac{k_\parallel}{\epsilon_s}E_{zs}\right)e^{-k_{zs}z_s}e^{i(k_\parallel x-\omega t)}. \quad (4)$$

The general details of these solutions can be found in the literature [14,16,20,21]. These are tailored to deal with the EF alone or the plasmon field (PF) alone. The associated wave numbers as the field crosses the interfaces $(s)\rightarrow(m)$ and $(m)\rightarrow(1)$, are the real $k_{z1}^2=(k_\parallel^2-\epsilon_1\omega^2/c^2)>0$, and $k_{zs}^2=(\epsilon_s\omega^2/c^2-k_\parallel^2)>0$; and the complex $k_{zm}^2=(k_\parallel^2-\epsilon_m\omega^2/c^2)>0$. At the vacuum side, expressed by Eq. (2), it will happen that $E_{x1}\simeq E_{z1}$. Thus any strength difference between these fields components will be related to a difference in their wave number only. That will be clear once we describe the associated potentials.

In a first approach we make the straightforward assumption that the existing solutions can be used, and we introduce a simplified picture in which the interactions of the orthogonal fields are "decoupled." The aim of the theory is then to superpose these two solutions on the assumption that they are weakly coupled, and that this coupling can be treated perturbatively. Thus we aim to represent: (1) that indeed the strengths of these fields compete against each other; and (2) under partial coupling, the EF's repulsive force would not be fully canceled by the attractive strength of the PF. This balancing of strengths against the other forces of the atomic mirror enables the construction of the desired potential well. We postpone until later a detailed analysis based on the different nature of these fields. We need to consider that the EF is a nonoscillatory decaying field whose presence has no dependence on the conductive properties of the thin layer and, even to some extent, does not have full dependence on the chosen illumination frequency. This is opposite to the conditions required for the PF. Also, since these fields are linearly independent, any interference between these is discarded.

In the enhanced evanescent potential, since the film thickness must be much lower than the optical wavelengths, diffraction effects will vanish. It would set up conditions for, otherwise, tunneling of photons from the dielectric-metal boundary up to the metal-vacuum boundary. As defined by Snell's law, the speed of the evanescent field will remain purely imaginary at the vacuum boundary [20]. Hence, above the metal surface, the oscillatory phase in the z-component of Eq. (1) equals zero and the field decays exponentially with no harmonic space-dependence as

$$E_e=E_{oe}e^{-2z/\Lambda_e}e^{-iwt}, \quad (5)$$

with $\Lambda_e=[(\omega/c)\sqrt{n^2\sin^2\theta-1}]^{-1}$ being the evanescent field's penetration depth into the vacuum, n is the refractive index of the dielectric prism, while E_{oe} is obtained from Eqs. (2)–(4) by applying the boundary conditions.

The choice of a frequency ω, blue-detuned with respect to the atomic transition ω_o (i.e., $\Delta_B=\omega-\omega_o$), is enough to produce the repulsive mirror potential on region I (see Fig. 1). The conditions to produce the plasmon potential are obtained by choosing the metal in region II (see Fig. 1) with the same thickness $(d\ll 2\pi c/\omega)$ as in region I, and such that the illumination frequency can excite its plasmon mode of characteristic frequency $\omega_{sp}^{II}=\omega_p^{II}/\sqrt{\epsilon_1+1}$. Here $(\omega_p^{II})^2=N_{II}e^2/(m_e\epsilon_o)$ is the region's II plasma frequency; where m_e and e are the electrons effective mass and charge, respectively, and N_{II} is the electron density per unit volume. These will set the conditions for photons to tunnel from the dielectric-metal interface up to the metal-surface where they trigger collective excitation of the conduction electrons, within the illumination area. These electrons will oscillate in a wavelike fashion, with their amplitude extended into the vacuum side up to a distance Λ_p. This is the so-called Kretschmann-Raether's surface plasmon polariton (SPP), i.e., the surface plasmon (SP) [20,21] of wave number $k_{sp}=(\omega/c)\sqrt{\epsilon_1\epsilon_m(\omega)/[\epsilon_1+\epsilon_m(\omega)]}$. The vacuum dielectric function is $\epsilon_1\simeq 1$. Whereas in regions I and II $(M=\mathrm{I},\mathrm{II})$ we have that $\epsilon_m^M(\omega)=1-(\omega_p^M)^2/[\omega(\omega+i\gamma_M)]\simeq 1-[(\omega_p^M)^2/\omega^2]$ is the complex Drude's dielectric function of the metallic thin film, where γ_M $(\simeq\tau_M^{-1}$, the inverse of the average free electron collision time) accounts for the metal's ohmic losses and hence for the length of propagation of the SP. The approximation in $\epsilon_m^M(\omega)$ is frequently taken when losses are negligible (i.e., $\gamma_M\approx 0$), as it could be for highly conductive materials (HCM). However, although we are using HCM, we

shall not take the approximation in our calculations; this is a macroscopic approximation that might not apply at the scale we are dealing with.

Taking into consideration all these parameters, and after reducing Eqs. (2)–(4), the associated plasmon field is

$$E_p = E_{op} e^{i(k_{sp}x-\omega t)} e^{-2z/\Lambda_p}. \tag{6}$$

The SP field oscillates along the x-axis; its distance of penetration into the vacuum is modulated by

$$\Lambda_{sp} = \left| \left[k_{sp}^2 - \frac{c^2}{\omega^2}\epsilon_1 \right]^{-1/2} \right|; \tag{7}$$

the operation $|\cdots|$ results from the dependence of k_{sp} with the complex valued function $\epsilon_m(\omega)=\mathrm{Re}\{\epsilon_m(\omega)\}+i\,\mathrm{Im}\{\epsilon_m(\omega)\}$, with $\mathrm{Re}\{\epsilon_m(\omega)\}<0$ at the ω_{sp} range.

The next step is to obtain the associated interaction potentials. Notice that to first order, the E_p field in Eq. (6) is similar to the one that is obtained from solving the Laplace equation in a dipole field configuration for a point above a metallic plate [22]. Therefore, and without loss of generality, we extrapolate that the related potential of interaction shall be $U_p=-(a_g/2)|E|^2$. This is an attractive potential, where a_g is the scalar atomic polarizability; for rubidium (Rb) this has the value of 5.3×10^{-39} m^2 c/V.

On the other hand, the EF has an average repulsive dipole potential U_{ef} whose associated strength $\boldsymbol{F}_{ef}=-\partial U_e/\partial z$, acts repulsing the atom. The general details can be found in, e.g., [16,23]. This potential is described as

$$U_e = \frac{\hbar\Delta_B}{2} \ln\left[1 + \frac{\Omega^2/2}{\Delta_B^2 + (\omega_o/2)^2} \right]; \tag{8}$$

here Ω is the Rabi frequency, and ω_o is the atom resonance frequency. For Rb this is $2\pi(6.02)$ MHz.

To combine these potentials in the way as we propose, we need to match optical and material parameters. Therefore the difference $\Delta_B>0$ should guarantee that Ω, ω, and ω_{sp}^{II} are suitable and sufficiently near each other so as to interactively overlap their distribution bands, while $\omega_p^I \gg \omega$.

Bearing in mind these conditions, we balance these potentials together with the gravitational one (mgz) aligned on the z-direction and with the attractive van der Waals potential (U_{vdW}), as described in [24,25]. Since the metal layer areas are well-defined and smaller than the laser spot size, the system of average forces is driven by localized systems. The result is localized potentials on top of regions I and II, respectively:

$$U^I = U_e + mgz - \frac{C_{\mathrm{vdW}}}{z^3}, \tag{9}$$

$$U^{II} = U_e + U_p + mgz - \frac{C_{\mathrm{vdW}}}{z^3}. \tag{10}$$

In order to calculate these potentials we choose silver for the enhancement of the EF, with ω_p^I that corresponds to a wavelength of nearly 200 nm. For the metal layer on region II we choose gold disks of $D=10$ μm diameter, with plasmon frequency (ω_p^{II}) around 520 nm wavelength, hence its surface plasmon wavelength is $\lambda_{SP}\simeq735$ nm. For both layers we assume 40 nm thickness. The illumination is with a cw laser beam at an angle of incidence of $\theta=60°$ and a power of 10 mW on a spot beam of 100 μm diameter. It is TM-polarized, parallel to the xz-plane. The illumination wavelength is blue-detuned at 760 nm with respect to the resonance for rubidium (780 nm). The prism is quartz with refractive index $n=1.47$. In the van der Waals potential, C_{vdW} is defined in terms of $a_{raw}=5.8\times10^{-49}$ kg m^5 s^{-2}, at an effective distance $\lambda_{eff}=907$ nm. Thus from this evaluation it results that the plasmon decay length is of about 570 nm and the evanescent decay length is $\simeq160$ nm; these are $\Lambda_{pl} \geqslant \Lambda_{ef}$ in the vacuum side. After the calculations we observe that the potential as we describe takes place when (1) SP wavelength is near $\simeq750$ nm, and (2) that simultaneously the PF amplitude is as big as 50% of the EF amplitude. In this way, we obtain the potential distribution displayed in Fig. 2 above the silver layer (region I) and Fig. 3 for the potential above the Au layer (region II).

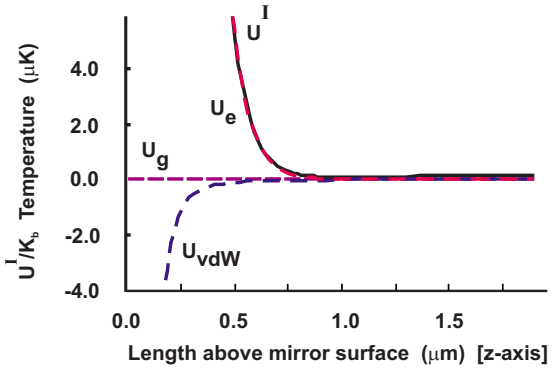

FIG. 2. (Color online) Display of the atomic mirror potential (U^I) distribution (solid line) above the Ag metallic layer. This potential is dominated by the U_e EF's potential strength over the van der Waals potential U_{vdW} and the gravitational potential (U_g).

After evaluating our system, we found that the potential well depth is slightly bigger than 7.0 μK and its center is slightly over 530 nm. This is above the metal surface. From Eqs. (2)–(4) one can obtain the decay length of the evanes-

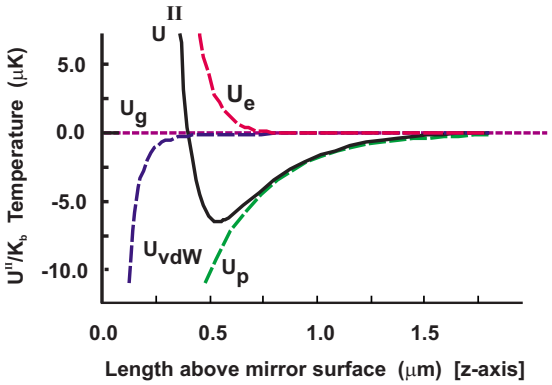

FIG. 3. (Color online) Display of the Potential well U^{II} (solid line) above the Au thin film. This time we added the plasmon field potential (U_p). This is evaluated accordingly with the parameters as is indicated in the main text. At 10 mW optical input power we compute a well's depth $\gtrsim7$ μK.

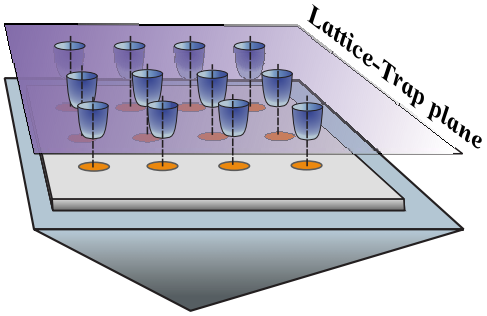

FIG. 4. (Color online) Schematic representation of one type of latticelike potential wells. This is for conceptual guidance. More complex systems including trap-to-trap communications via channel plasmon waveguides are within the reach of this concept.

cent field above the prism-Au system, in our case it is almost 160 nm. Also, by assuming a flat-top illumination beam profile, the valley of the potential well is also flat. Instead, when taking a Gaussian beam profile, a small depression arises at the bottom of the potential well; however, its amplitude is negligible compared with the well's depth, and thus would not affect the general results. Since we consider all the materials as isotropic, and these are illuminated well below their saturation limit, effects like zero-point fluctuations [26] will not affect our results.

The trap resulting from the configuration described, once it is set up, will be ready to be fed with cold atoms [27]. The expected method to realize these kinds of traps is by applying micro- and nanolithography and/or thin film deposition techniques to replicate this several times and then tailor latticelike distributions (we display a schematic example in Fig. 4). As it is seen from the calculations, it is feasible to gain control of accessible parameters to tailor potential wells of this type. Under reasonable conditions the potential can be replicated to obtain a latticelike structure. The viability of its actual realization depends more on practical possibilities than on physical conditions. Indeed, there is a number of points which must be clarified, from the theoretical and practical viewpoints. We intend to pursue our work on the present subject. This time, our sole purpose is to instigate the viability of this concept, with the hint that this could be the way to link the atom trap and the atom chip with advances in the plasmonics field [28].

[1] S. Chu, J. E. Bjorkholm, A. Ashkin, and A. Cable, Phys. Rev. Lett. **57**, 314 (1986).
[2] A. L. Migdall, J. V. Prodan, W. D. Phillips, T. H. Bergeman, and H. J. Metcalf, Phys. Rev. Lett. **54**, 2596 (1985).
[3] C. N. Cohen-Tannoudji, Rev. Mod. Phys. **70**, 707 (1998).
[4] J. D. Miller, R. A. Cline, and D. J. Heinzen, Phys. Rev. A **47**, R4567 (1993).
[5] D. Jaksch, H. J. Briegel, J. I. Cirac, C. W. Gardiner, and P. Zoller, Phys. Rev. Lett. **82**, 1975 (1999).
[6] J. Schmiedmayer, R. Folman, and T. Carlarco, J. Mod. Opt. **49**, 1375 (2002).
[7] A. Haase, D. Cassettari, and B. H. J. Schmiedmayer, Phys. Rev. A **64**, 043405 (2001).
[8] R. Folman, P. Kruger, D. Cassettari, B. Hessmo, T. Maier, and J. Schmiedmayer, Phys. Rev. Lett. **84**, 4749 (2000).
[9] C. Henkel and M. Wilkens, Europhys. Lett. **47**, 414 (1999).
[10] J. Fortagh, H. Ott, S. Kraft, A. Gunther, and C. Zimmermann, Phys. Rev. A **66**, 041604(R) (2002).
[11] P. K. Rekdal, S. Scheel, P. L. Knight, and E. A. Hinds, Phys. Rev. A **70**, 013811 (2004).
[12] Y. B. Ovchinnikov, I. Manek, and R. Grimm, Phys. Rev. Lett. **79**, 2225 (1997).
[13] M. B. Crookston, P. M. Baker, and M. P. Robinson, J. Phys. B **38**, 3289 (2005).
[14] M. Hammes, D. Rychtarik, B. Engeser, H. C. Nagerl, and R. Grimm, Phys. Rev. Lett. **90**, 173001 (2003).
[15] R. J. Cook and R. K. Hill, Opt. Commun. **43**, 258 (1982).
[16] C. R. Bennett, J. B. Kirk, and M. Babiker, Phys. Rev. A **63**, 033405 (2001).
[17] H. F. Ghaemi, T. Thio, D. E. Grupp, T. W. Ebbesen, and H. J. Lezec, Phys. Rev. B **58**, 6779 (1998).
[18] L. H. Ford (unpublished).
[19] E. Moreno, A. I. Fernández-Domínguez, J. Ignacio Cirac, F. J. Garcí-Vidal, and L. Martín-Moreno, Phys. Rev. Lett. **95**, 170406 (2005).
[20] A. V. Zayats, I. I. Smolyaninov, and A. A. Maradudin, Phys. Rep. **408**, 131 (2005).
[21] H. Raether, *Surface Plasmons on Smooth and Rough Surfaces and on Gratings* (Springer-Verlag, Berlin, 1998).
[22] W. A. van Wijngaarden and J. Clarke, Can. J. Phys. **76**, 305 (1998).
[23] T. Esslinger, M. Weidenmuller, A. Hammerich, and T. W. Hanch, Opt. Lett. **18**, 450 (1993).
[24] F. Shimizu, Phys. Rev. Lett. **86**, 987 (2001).
[25] A. Landragin, J.-Y. Courtois, G. Labeyrie, N. Vansteenkiste, C. I. Westbrook, and A. Aspect, Phys. Rev. Lett. **77**, 1464 (1996).
[26] I. I. Smolyaninov, Phys. Rev. Lett. **94**, 057403 (2005).
[27] Y. B. Ovchinnikov, I. Manek, and R. Grimm, Phys. Rev. Lett. **79**, 2225 (1997).
[28] S. I. Bozhevolnyi, V. S. Volkov, E. Devaux, and T. W. Ebbesen, Nature (London) **440**, 508 (2006).